

## THE SLOAN DIGITAL SKY SURVEY PHOTOMETRIC SYSTEM

M. FUKUGITA<sup>1</sup>

Institute for Advanced Study, Princeton, New Jersey 08540  
 Electronic mail: fukugita@sns.ias.edu

T. ICHIKAWA

Kiso Observatory, University of Tokyo, Kiso-gun, Nagano 397-01, Japan  
 Electronic mail: ichikawa@kiso.ioa.s.u-tokyo.ac.jp

J. E. GUNN

Princeton University Observatory, Princeton, New Jersey 08544  
 Electronic mail: jeg@astro.princeton.edu

M. DOI AND K. SHIMASAKU

Department of Astronomy, University of Tokyo, Tokyo 113, Japan  
 Electronic mail: doi@astron.s.u-tokyo.ac.jp; shimasaku@astron.s.u-tokyo.ac.jp

D. P. SCHNEIDER

Department of Astronomy, Pennsylvania State University, University Park, Pennsylvania 16802  
 Electronic mail: dps@miffy.astro.psu.edu

Received 1995 September 11; revised 1995 December 20

## ABSTRACT

This paper describes the Sloan Digital Sky Survey photometric system, a new five-color ( $u'g'r'i'z'$ ) wide-band CCD system with wavelength coverage from 3000 to 11 000 Å. The zero points will be based on an updated version of the spectrophotometric  $AB_v$  system. This updated calibration, designated as  $AB_{95}$ , is presented in this paper. © 1996 American Astronomical Society.

## 1. INTRODUCTION

This paper describes the photometric system to be used for the Sloan Digital Sky Survey (SDSS). The zero point of this photometric scheme is the  $AB_v$  system of Oke & Gunn (1983, hereafter referred to as OG); this convention allows immediate conversion from magnitudes to physical fluxes. To improve the accuracy of the transformations, we introduce an improved absolute calibration, which we designate as  $AB_{95}$ . This paper is primarily intended to facilitate work in anticipation of survey data. Observations of the secondary standard stars for the SDSS system began in the spring of 1996; a list of SDSS standard stars and their magnitudes will be published in late 1997.

The system comprises five color bands ( $u'$ ,  $g'$ ,  $r'$ ,  $i'$ , and  $z'$ ) that divide the entire range from the atmospheric ultraviolet cutoff at 3000 Å to the sensitivity limit of silicon CCDs at 11 000 Å into five essentially nonoverlapping pass bands. The five filter curves are displayed in Fig. 1. The filters have the following properties:  $u'$  peaks at 3500 Å with a full width at half maximum of 600 Å,  $g'$  is a blue-green band centered at 4800 Å with a width of 1400 Å,  $r'$  is the red passband centered at 6250 Å with a width 1400 Å,  $i'$  is a far

red filter centered at 7700 Å with a width of 1500 Å, and  $z'$  is a near-infrared passband centered at 9100 Å with a width of 1200 Å; the shape of the  $z'$  response function at long wavelengths is determined by the CCD sensitivity.

While the names of these bands are similar to those of the Thuan & Gunn (TG) photometric system (Thuan & Gunn 1976; Wade *et al.* 1979; Schneider *et al.* 1983), the SDSS system is substantially different from the TG bands. The most salient feature of the SDSS photometric system is the very wide bandpasses used, even significantly wider than that of the standard Johnson–Morgan–Cousins system (Johnson & Morgan 1953; Cousins 1978). These filters ensure high efficiency for faint object detection and essentially cover the entire accessible optical wavelength range. Prospective users of the system for other purposes should note, however, that the large widths can introduce significant flat-fielding problems, especially with older back-illuminated CCDs used in “staring” mode in the red and near-infrared bands; in this situation caution must be exercised in their use.

The filter responses are in general determined by a sharp-cutoff long-pass glass filter onto which is coated a short-pass interference film, and thus exhibit wide plateaus terminated with fairly sharp edges. The exceptions are the  $u'$  filter (the passband is defined by the glass on both sides and it is much narrower than the others) and the  $z'$  filter (no long wavelength cutoff). The division of the passbands is designed to exclude the strongest night-sky lines of O I  $\lambda$ 5577 and Hg I

<sup>1</sup>Yukawa Institute, Kyoto University, Kyoto 606, Japan; Electronic mail: fukugita@jpnypitp.yukawa.kyoto-u.ac.jp

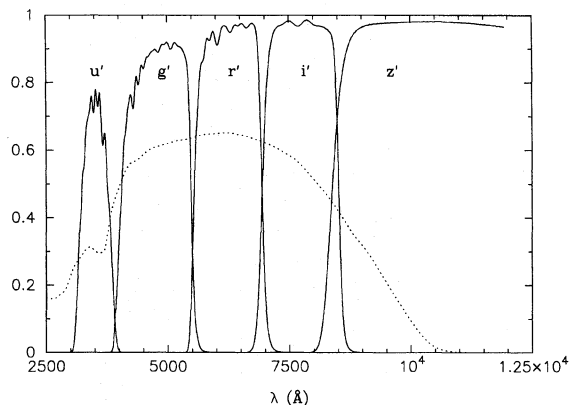


FIG. 1. Transmission of the  $u'$ ,  $g'$ ,  $r'$ ,  $i'$ ,  $z'$  filters. Redleaks shortward of 11 000 Å are not shown. The dotted curve is the quantum efficiency of a thinned, UV-coated SiTe CCD; this is the detector that is used in the definition of the SDSS system.

$\lambda 5460$ , as is the case with the TG photometric system. The  $u'$  band response is similar to TG  $u$  and Strömgren  $u$  in that the bulk of the response is shortward of the Balmer discontinuity; this produces a much higher sensitivity (combining with  $g'$ ) to the magnitude of the Balmer jump at the cost of lower total throughput. Proper consideration of photon noise clearly indicates that this is to be preferred to a wider band with dilution by redder light.

The SDSS system will be defined by observations with the SDSS "Monitor Telescope," a 60 cm reflector located at Apache Point Observatory. The detector is a thinned, back-illuminated, UV-antireflection-coated CCD device procured from Scientific Imaging Technologies, Inc. (SiTe). In the survey camera, the  $u'$  filters are used in conjunction with the same UV-coated chips as is used in the Monitor Telescope, the  $g'$ ,  $r'$ , and  $i'$  with normal visual-band antireflection-coated thinned devices, and the  $z'$  filters with thick, front-illuminated CCDs.

A novel (and to our mind, long overdue) feature of the SDSS photometric system is the attempt to place the zero points on the spectrophotometric  $AB$  magnitude system. The  $AB$  system is a monochromatic ( $f_\nu$ ) system first introduced by Oke in 1969 with a provisional calibration, designated  $AB_{69}$ . This system was widely used in the spectrophotometric community in the 1970s; an improved calibration was presented by OG as the system  $AB_{79}$ . In the  $AB_{79}$  system the spectrophotometric energy distributions (SEDs) of the four F subdwarfs BD+17°4708, BD+26°2606, HD 19445, and HD 84937, the absolute fluxes of which are calibrated against the absolute flux of the continuum of  $\alpha$  Lyr, are taken as the defining monochromatic magnitude standards. The spectra of these cool, metal-deficient stars are much simpler than those of A dwarfs with their very strong, wide Balmer lines and large Balmer discontinuity. The moderately flat SEDs and weak lines of the F subdwarfs also minimize the errors of synthetic magnitudes that arise from uncertainties in the details of the shape of system response functions.

The great advantage of the  $AB$  magnitude system is that

TABLE 1. Elements of SDSS filters.

filter	glass	coating
$u'$	1mm UG11 + 1mm BG38 + 3mm quartz	coating that suppresses 6600–8200Å
$g'$	2mm GG400 + 3mm BG38	short-pass coating cut off at 5500Å
$r'$	4mm OG550 + 1mm BK7	short-pass coating cut off at 7000Å
$i'$	4mm RG695 + 1mm BK7	short-pass coating cut off at 8500Å
$z'$	4mm RG830 + 1mm BK7	

the magnitude is directly related to physical units; OG defined the magnitude by

$$AB_\nu = -2.5 \log f_\nu (\text{ergs s}^{-1} \text{cm}^{-2} \text{Hz}^{-1}) - 48.60, \quad (1)$$

where  $f_\nu$  is the flux per unit frequency from the object, so

$$f_\nu (\text{Jy}) = 3631 \text{ dex}(-0.4AB_\nu). \quad (2)$$

Since the work of OG, much effort has been expended in improving the SED of  $\alpha$  Lyr (see Hayes 1985, hereafter referred to as H85; Castelli & Kurucz 1994). The SEDs of the four  $AB_{79}$  subdwarfs have also been revised by Oke (1990). In this paper we update  $AB_{79}$  by recalibrating the flux of the four subdwarf standards using the best modern data of the  $\alpha$  Lyr flux and the four OG subdwarfs; we call the new system  $AB_{95}$ .

## 2. RESPONSE FUNCTIONS

### 2.1 Filters

The physical composition of the filters is given in Table 1. The filters are made from one or two Schott color glass elements together with a multilayer interference film coating on one glass-air surface.

The  $u'$  filter is made of a combination of UG11, which cuts off the long-wavelength side, and BG38, which cuts off the short side, with an interference film coating that suppresses the red leak in the glass filters in the 6700–7400 Å region; without the coating, one would expect a maximum transmission of about 7% in a narrow region around 7000 Å. The coating is devised to suppress the leakage by a large factor ( $\geq 1 \times 10^4$ ) at around 7100 Å, and by a factor  $\geq 100$  between 6650 and 8000 Å, so that the net maximum leakage does not exceed  $3 \times 10^{-4}$  for all wavelengths between 6000 and 10 000 Å when combined with color glasses. This coating also impairs the transmission in the passband slightly.

The  $g'$  filter is constructed of GG400, the long-pass element, and a short-pass interference coating that cuts off at 5500 Å. This coating is made simpler by the inclusion of an extra BG38 glass element, which blocks the filter in the red but is quite transparent in the passband.

The  $r'$  and  $i'$  filters consist of long-pass OG550 and RG695 glasses, in combination with short-pass interference coatings which cut off at 7000 and 8500 Å, respectively. There are no satisfactory red blocking glasses for these filters, and a large red leak appears at wavelengths longer than 11 000 Å for  $r'$  and  $i'$ , but ordinary silicon CCDs have so little response at these wavelengths that the errors introduced are very small. We discuss the performance in more detail below.

For the  $z'$  band, the short-wavelength side is defined by RG830, and the long-wavelength side is open, so the re-

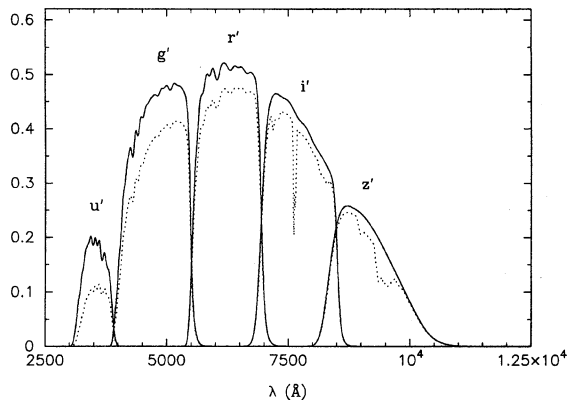


FIG. 2. Response function of the SDSS photometric system, using a UV-coated thinned CCD. Dashed curves indicate the response function including atmospheric transmission at 1.2 airmasses at the altitude of Apache Point Observatory.

sponse is essentially defined by the CCD. These filters are brought to 5 mm thickness by adding a neutral glass element (BK7 or quartz), so that all filters have approximately the same optical depth and can be incorporated into the converging beam of a Monitor Telescope camera. Of course, this does not induce any effect on the defined passbands.

The interference coatings are applied by Asahi Spectra Ltd., Tokyo. The manufactured filter transmission curves are shown in Fig. 1, as measured with a Shimadzu UV-3100PC spectrometer at National Astronomical Observatory in Tokyo. High peak transmission (over 95% for  $r'i'z'$  and more than 90% for  $g'$ ) is attained with efficient antireflection coatings. For the  $u'$  band, we obtain 78% transmission at its peak. For all the filters, red leaks are suppressed to transmission levels of  $\leq 0.1\%$  for wavelengths shortward of 10 500 Å, the effective cutoff of the CCD response function.

The quantum efficiency of a thinned back-illuminated SiTe CCD with a UV antireflection coating (the chip intended for use in the Monitor Telescope) at a temperature of 180 K is also depicted in the same figure. This curve was constructed by modulating the room-temperature quantum efficiency curve measured at SiTe so that it reproduced our measurements at 180 K for 14 discrete wavelengths. The efficiency is flat at 60% for 4000–7000 Å; 30% efficiency is attained in the ultraviolet region.

The system response functions are shown in Fig. 2. The response curves include the filter transmission, the quantum efficiency for the thinned, UV-coated CCD, and the reflectivities of two aluminium surfaces (Hass 1965; see also Shiles *et al.* 1980; Magrath 1994). The curves including atmospheric extinction at 1.2 airmasses, based on the standard Palomar monochromatic extinction tables scaled to the altitude of Apache Point Observatory (2800 m), are also shown. Extinction in the atmospheric  $O_2$  and water vapor is calculated with a square-root law. Machine-readable versions of all response curves can be obtained by contacting the first author.

The effective wavelengths for each filter, both with (1.2 airmass) and without atmospheric extinction, are tabulated in

Table 2a. Characteristics of the SDSS photometric system (1.2 airmass)

	$u'$	$g'$	$r'$	$i'$	$z'$
$\lambda_{\text{eff}}^{(1)}$ (Å)	3557	4825	6261	7672	9097
$\lambda_{\text{eff}}^{(2)}$ (Å)	3524	4714	6182	7592	9003
$\lambda_{\text{eff}}^{(3)}$ (Å)	3540	4770	6222	7632	9049
FWHM (Å)	599	1379	1382	1535	1370
$\sigma^{(4)}$	0.0556	0.0880	0.0652	0.0592	0.0586
$\Delta\lambda^{(5)}$ (Å)	463	988	955	1064	1248
$Q^{(6)}$	0.0181	0.110	0.101	0.0766	0.0354

Table 2b. The same as (a), but without atmospheric extinction

	$u'$	$g'$	$r'$	$i'$	$z'$
$\lambda_{\text{eff}}^{(1)}$ (Å)	3522	4803	6254	7668	9114
$\lambda_{\text{eff}}^{(2)}$ (Å)	3487	4690	6174	7589	9024
$\lambda_{\text{eff}}^{(3)}$ (Å)	3504	4747	6214	7628	9068
FWHM (Å)	634	1409	1388	1535	1409
$\sigma^{(4)}$	0.0577	0.0891	0.0654	0.0588	0.0575
$\Delta\lambda^{(5)}$ (Å)	476	996	957	1056	1227
$Q^{(6)}$	0.0340	0.134	0.113	0.0837	0.0401

Table 2c. Johnson-Morgan-Cousins system

	$U$	$B$	$V$	$R_c$	$I_c$
$\lambda_{\text{eff}}^{(1)}$ (Å)	3652	4448	5505	6581	8059
$\lambda_{\text{eff}}^{(2)}$ (Å)	3617	4364	5437	6410	7980
$\lambda_{\text{eff}}^{(3)}$ (Å)	3635	4405	5470	6492	8020
FWHM (Å)	524	1008	826	1576	1543
$\sigma^{(4)}$	0.0566	0.0801	0.0642	0.0940	0.0574
$\Delta\lambda^{(5)}$ (Å)	484	831	826	1437	1084
$Q^{(6)}$	—	—	—	—	—

Note — 1) effective wave length. 2) inverse of effective frequency.  
3) defined by eq.(3). 4) fractional bandwidth defined by eq.(4).  
5) FWHM of an effective Gaussian bandpass derived from  $\sigma$ .  
6) flux sensitivity quantity defined by eq.(5).

Table 2 (those for the Johnson–Morgan–Cousins system are also listed for comparison). In any filter of finite width, the effective wavelength cannot be uniquely defined; we present the effective wavelengths of the SDSS filters as defined by several extant conventions. The first row gives the wavelength-weighted average, the second contains the frequency-weighted average (written as  $c\nu_{\text{eff}}^{-1}$ ), and the third lists the effective wavelength as defined by Schneider *et al.* (1983):

$$\lambda_{\text{eff}} = \exp \left[ \frac{\int d(\ln \nu) S_\nu \ln \lambda}{\int d(\ln \nu) S_\nu} \right], \quad (3)$$

which is in some sense halfway between an effective wavelength and an effective frequency. (This definition has the attractive feature that  $\lambda_{\text{eff}}$  and the similarly defined effective frequency are consistent with each other.) Here and below,  $S_\nu$  is the system quantum efficiency; this includes atmospheric absorption. In Table 2 we also present the rms fractional widths of the filters  $\sigma$ , defined as

$$\sigma = \left[ \frac{\int d(\ln \nu) S_\nu [\ln(\lambda/\lambda_{\text{eff}})]^2}{\int d(\ln \nu) S_\nu} \right]^{1/2}, \quad (4)$$

and the flux sensitivity quantity  $Q$ , defined as

$$Q = \int d(\ln \nu) S_\nu. \quad (5)$$

The former is useful in calculating the sensitivity of the effective wavelength to spectral slope changes:  $\delta\lambda_{\text{eff}} = \lambda_{\text{eff}} \sigma^2 \delta n$ , where  $n$  is the local power-law index of the

TABLE 3. Calculated atmospheric extinction coefficients.

$k_r$	$k_{ug}$	$k_{gr}$	$k_{ri}$	$k_{iz}$
0.093 $[(r' - i') \leq 0.5]$	0.399 $[(u' - g') \leq 1.3]$	0.090	0.013	-0.032
0.091 $[(r' - i') > 0.5]$	0.360 $[(u' - g') > 1.3]$			
$k'_r$	$k'_{ug}$	$k'_{gr}$	$k'_{ri}$	$k'_{iz}$
-0.006 $[(r' - i') \leq 0.5]$	-0.029 $[(u' - g') \leq 1.3]$	-0.015	-0.003	-0.009
-0.002 $[(r' - i') > 0.5]$	0.000 $[(u' - g') > 1.3]$			

SED ( $f_\nu \sim \nu^n$ ), and the effective band width (full width at half maximum of an effective Gaussian for  $n=0$ ) is given by  $2(2 \ln 2)^{1/2} \sigma \lambda_{\text{eff}}$ . Equation (5) allows quick approximate calculations for the response of a system to a source of known flux:

$$N_e = A t Q f_{\nu_{\text{eff}}} h^{-1}, \quad (6)$$

where  $N_e$  is the number of photoelectrons collected from a system of effective area  $A$  integrating for a time  $t$  on a source of flux  $f_\nu$ ;  $h$  is the Planck constant. Characteristics of the standard Johnson–Morgan–Cousins photometric system are also shown in Table 2 for comparison. The full widths at half maximum for the SDSS response functions are about 1.5 times those of the Johnson–Morgan passbands (Johnson & Morgan 1953), except for  $u'$ .

The charge deposited in a CCD pixel and subsequently measured by the data system is just proportional to the *photon* flux times the system quantum efficiency, integrated over the passband, and the natural magnitude is just  $-2.5$  times the common logarithm of that charge. We thus define the broadband  $AB$  magnitude by

$$m = -2.5 \log \frac{\int d(\log \nu) f_\nu S_\nu}{\int d(\log \nu) S_\nu} - 48.60, \quad (7)$$

where  $f_\nu$  is the energy flux per unit frequency incident on the atmosphere. If one knew the spectrum of a source and the system response perfectly, this expression would reproduce the natural magnitude system exactly. This remark is probably pedantic, but please note that there is *no* freedom in the definition of the integrand aside from an arbitrary constant multiplier if one is to correctly reproduce the response measured from sources with arbitrary spectral shapes.

## 2.2 Atmospheric Extinction

We write the color extinction equations for  $r'$  and four color indices  $(u' - g')$ ,  $(g' - r')$ ,  $(r' - i')$ , and  $(i' - z')$ , as

$$\begin{aligned} r' &= r'_0 + [k_r + k'_r(r' - i')]Z, \\ (g' - r') &= (g' - r')_0 + [k_{gr} + k'_{gr}(g' - r')]Z, \\ (u' - g') &= (u' - g')_0 + [k_{ug} + k'_{ug}(u' - g')]Z, \\ (r' - i') &= (r' - i')_0 + [k_{ri} + k'_{ri}(r' - i')]Z, \\ (i' - z') &= (i' - z')_0 + [k_{iz} + k'_{iz}(i' - z')]Z, \end{aligned} \quad (8)$$

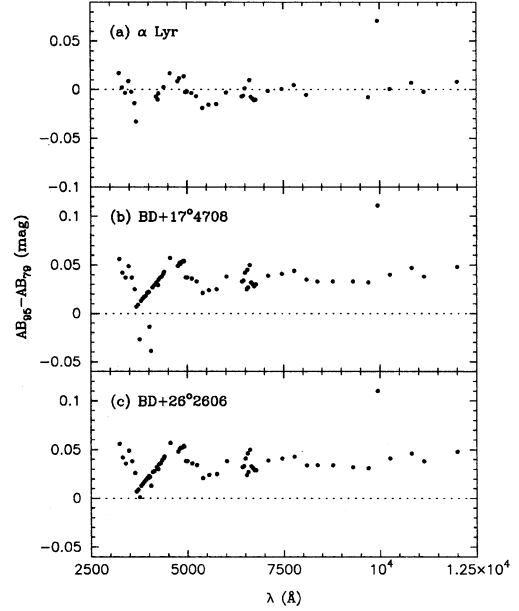


FIG. 3. (a) Offset of the SED of  $\alpha$  Lyr between  $AB_{95}$  (=H85) and  $AB_{79}$  (=OG). (b) Offset of  $AB_{95}$  calibration against  $AB_{79}$  for BD+17°4708. (c) As (b), but for BD+26°2606.

where the magnitudes and color indices with suffix 0 denote values corrected for extinction and those without suffixes the observed magnitude, and  $Z$  is the airmass.

Table 3 gives the expected values for the extinction coefficients using the standard Palomar monochromatic extinction tables scaled to the altitude of Apache Point Observatory. The magnitude of the second-order color terms indicates that they cannot be ignored if one desires an accuracy of better than about 0.02 mag over a wide color range.

The magnitudes we discuss in the following sections are all extinction-free magnitudes. We omit the subscript 0 for simplicity of notations.

## 3. THE $AB_{95}$ MAGNITUDE SYSTEM

### 3.1 Definition

The  $AB_{79}$  system was introduced by OG partly to refine the calibration of the older system but largely to present a set of well-calibrated secondary standards with simple spectra faint enough to be used with large telescopes. F subdwarfs, which had already been in use for some years for this purpose, seem ideal. They have reasonably flat spectra, and the most metal-deficient ones have very weak absorption features. Since absolute calibration work has centered on  $\alpha$  Lyr (there are no bright F subdwarfs), it is necessary to obtain the absolute calibration of these stars by calibrating against the absolute fluxes of  $\alpha$  Lyr in the continuum.

OG used the compilation of Hayes & Latham (1975) for the relative SED of  $\alpha$  Lyr, modified slightly by demanding a better fit to the Kurucz model atmosphere, and interpolating in the difficult region near 4000 Å using data from very hot subdwarfs. They normalized the SED at 5480 Å with the flux measured by Oke & Schild (1970) (Oke & Schild's zero



TABLE 4. Offset of the broadband magnitude  $AB_{95}-AB_{79}$  for  $\alpha$  Lyr.

$\Delta u'$	$\Delta g'$	$\Delta r'$	$\Delta i'$	$\Delta z'$	$\Delta U$	$\Delta B$	$\Delta V$	$\Delta Rc$	$\Delta Ic$
-0.004	-0.000	-0.007	-0.000	0.020	-0.009	0.001	-0.009	-0.005	0.000

point at 5480 Å appears to have an error in the interpolation of the SED; their value is closer to Hayes & Latham's value than would actually be obtained from the Oke-Schild SED). OG defined the  $AB$  magnitude so that this flux corresponds to  $V=0.03$  at this specific wavelength. This led to the definition given in Eq. (1).

Since the work of OG, a number of studies have been made of the  $\alpha$  Lyr SED, both for absolute flux and for the relative flux distribution. The most recent compilation of the  $\alpha$  Lyr SED is given by H85. The relative SED given by H85 agrees very well with that of Castelli & Kurucz (1994) based on a detailed stellar atmosphere calculation, except for small discrepancies in the Balmer absorption lines and in the Paschen region. H85 also updated the absolute flux; his best estimate of the flux at 5556 Å is  $f_\lambda=3.44\pm0.05\times10^{-9}$  ergs cm $^{-2}$  s $^{-1}$  Å $^{-1}$ , which is 1.5% larger than Hayes & Latham's (1975) value and 2.4% larger than that found by Oke & Schild. Here we adopt the value of H85. With the use of the H85 SED, the flux at 5480 Å is

$$f_\nu = 3.59 \times 10^{-20} \text{ ergs}^{-1} \text{ cm}^{-2} \text{ Hz}^{-1}. \quad (9)$$

This value is 1.6% (0.018 mag) larger than the zero point of the  $AB_{79}$  calibration. The offset between the Hayes SED and that of OG is shown in Fig. 3; this leads to offsets in the broad band colors as shown in Table 4. While the SED itself suffers from significant changes from  $AB_{79}$ , the changes in the broadband colors cancel out to a very large extent upon integration over the band, and the net effect is rather small.

We have decided to retain the definition (1) for the  $AB$  magnitude and absorb the changes in the zero points for the calibrating SEDs. With our revision, we then have  $AB=0.012$  for  $\alpha$  Lyr at 5480 Å. The broadband Johnson-Morgan  $V$  magnitude of  $\alpha$  Lyr is calculated to be  $V_{AB}=0.019$ , using the response functions of Azusienis & Straizys (1969, hereafter referred to as AS69). (Note that the  $V$  magnitude can be calculated fairly accurately from the SED of  $\alpha$  Lyr, since the star does not contain any strong absorption lines in this color band.) This synthetic value<sup>2</sup> is within 0.01 mag of the measured  $V$  magnitude (0.03) of  $\alpha$  Lyr; while it would be desirable to define the zero point of the  $AB$  system such that the synthetic  $V$  magnitude had no offset with respect to the observational  $V$  system, we feel that it is better to retain the original definition of the relation between  $AB$  and absolute fluxes. Uncertainties in the response function and observational errors in any case make any attempt to do very much better suspect, and we leave it as it is.

OG have measured the brightness of BD+17°4708 relative to  $\alpha$  Lyr, and tabulated the flux of the former on the  $AB_{79}$  system. They also measured fluxes of the other three

TABLE 5. Comparison of observed and synthesized magnitudes for the four dwarfs.

	$V_{\text{obs}}$	$V_{\text{syn}}$	$\Delta V$	$B_{\text{obs}}$	$B_{\text{syn}}$	$\Delta B$
BD+17°4708	$9.470 \pm 0.011$	9.43	0.04	$9.912 \pm 0.015$	9.88	0.03
BD+26°2606	$9.732 \pm 0.008$	9.69	0.04	$10.157 \pm 0.009$	10.14	0.02
HD19445	$8.057 \pm 0.019$	8.01	0.05	$8.515 \pm 0.021$	8.48	0.03
HD84937	$8.322 \pm 0.022$	8.29	0.03	$8.714 \pm 0.028$	8.68	0.03

Note – Observed magnitudes are taken from Mermilliod (1991), and the errors are dispersion among many (11-20) measurements.

subdwarf standards, BD+26°2606, HD 19445, and HD 84937 relative to BD+17°4708. Oke (1990) remeasured the SED of these four subdwarfs and updated their fluxes. We have recalibrated the fluxes using the H85 SED for  $\alpha$  Lyr. This is essentially the system proposed for  $AB_{95}$  except for a small zero-point shift, which we discuss in the next section.

### 3.2 Accuracy of the $AB$ Magnitude Zero Point

The errors in the present  $AB$  magnitude system arise from (1) errors in the measured relative SED of  $\alpha$  Lyr, (2) errors in the SED of BD+17°4708 (and the other three subdwarf standards) relative to that of  $\alpha$  Lyr, (3) errors in the shapes of the response functions, and (4) the absolute flux normalization of  $\alpha$  Lyr. The error arising from (1) is probably about 0.01 mag (except for the  $z'$  band which falls in the Paschen region) from a comparison of H85 with Castelli & Kurucz (1994). For (2), Oke (1990) quotes 0.02 mag. H85 estimates the error of (4) to be 0.015 mag. If an accuracy of 0.02 mag is achieved for (3) (this is the level achieved for the Johnson-Morgan photometric bands; see AS69; Buser 1978), the overall error will be about 0.03 mag including the normalization error.

For verification we have compared observed  $V$  and  $B$  magnitudes with the synthetic magnitudes for the four subdwarfs (see Table 5). The data are taken from the compilation of Mermilliod (1991). All four stars have been measured 10–20 times, and Mermilliod lists the average of these observations. The result is  $\langle \Delta V \rangle_{\text{synthetic-observed}} = -0.041 \pm 0.005$  (Note that the error from (4) does not come into this analysis). While this error is roughly consistent with what is expected, there seems to be a systematic offset of 0.04 mag (synthetic magnitude is brighter). A similar offset between the synthetic and observed magnitude is also seen in the  $B$  band. Similar offsets were already noted by Oke (1990). The origin of this systematic error is unknown, but is likely associated with the difficulty of tying a star as bright as  $\alpha$  Lyr to the faint standards with photoelectric pulse-counting techniques; OG were forced to go through one level of intermediate standards to tie the two together. We have chosen here to deal with the problem by making the subdwarfs all fainter by 0.04 mag at all wavelengths (we have weighted the  $V$  offsets more heavily than the  $B$  ones, but the offset is in any case likely to be between 0.03 and 0.04). We do not, of course, know in detail that the error is not wavelength dependent, but we are encouraged by the good agreement between the  $B$  and  $V$  offsets. We note parenthetically that it is of great importance to attempt to measure the ratio of the flux of BD+17°4708 to that of  $\alpha$  Lyr with a truly linear system at a variety of wavelengths as soon as possible.

<sup>2</sup>Here and hereafter we refer to the magnitude calculated by integrating the SED with the filter response function as synthetic magnitude.

TABLE 6. Updated calibration of the four F subdwarfs and  $\alpha$  Lyr.

$\lambda$	$\alpha$ Lyr	BD+17°4708	BD+26°2606	HD19445	HD84937
3080	1.283	11.015	11.215	9.536	9.737
3160	1.251	10.927	11.127	9.446	9.665
3240	1.235	10.853	11.053	9.365	9.597
3320	1.194	10.759	10.976	9.273	9.521
3400	1.163	10.698	10.901	9.203	9.457
3480	1.149	10.648	10.853	9.150	9.417
3560	1.116	10.572	10.786	9.075	9.346
3594	1.104	10.541	10.751	9.041	9.321
3607	1.099	10.540	10.750	9.040	9.320
3640	1.080	10.511	10.722	9.003	9.293
3680	1.050	10.457	10.675	8.950	9.248
3705	1.026	10.438	10.663	8.952	9.226
3713	1.009	10.430	10.657	8.927	9.217
3715	1.004	10.428	10.656	8.925	9.212
3720	0.994	10.433	10.658	8.926	9.212
3723	0.988	10.412	10.642	8.957	9.197
3726	0.977	10.407	10.637	8.957	9.187
3736	0.909	10.388	10.638	8.903	9.163
3741	0.876	10.378	10.628	8.893	9.153
3755	0.783	10.299	10.549	8.874	9.074
3759	0.754	10.279	10.539	8.854	9.049
3777	0.630	10.190	10.470	8.780	8.940
3782	0.592	10.210	10.460	8.760	8.930
3780	0.494	10.174	10.405	8.742	8.948
3814	0.383	10.082	10.352	8.692	8.842
3822	0.338	10.182	10.392	8.712	8.872
3840	0.219	10.170	10.406	8.757	8.923
3860	0.104	9.964	10.244	8.619	8.744
3866	0.074	10.034	10.274	8.614	8.739
3880	0.030	10.133	10.371	8.717	8.888
3905	0.004	9.994	10.256	8.606	8.746
3911	-0.028	9.966	10.239	8.601	8.696
3920	-0.074	10.138	10.309	8.719	8.832
3947	-0.036	10.028	10.198	8.608	8.688
3953	-0.022	10.008	10.243	8.623	8.713
3960	-0.011	10.139	10.337	8.709	8.862
3980	-0.028	10.111	10.337	8.701	8.861
3993	-0.129	9.880	10.160	8.510	8.640
4000	-0.180	9.911	10.165	8.521	8.688
4020	-0.260	9.851	10.137	8.481	8.621
4060	-0.222	9.833	10.115	8.453	8.613
4080	-0.104	9.864	10.104	8.454	8.634
4100	-0.003	9.966	10.209	8.552	8.751
4120	-0.091	9.826	10.086	8.444	8.611
4140	-0.194	9.817	10.087	8.400	8.599
4160	-0.246	9.818	10.068	8.423	8.598
4200	-0.244	9.796	10.051	8.406	8.586
4240	-0.240	9.786	10.033	8.401	8.571
4260	-0.229	9.794	10.042	8.412	8.581
4270	-0.221	9.784	10.034	8.376	8.569
4300	-0.135	9.865	10.095	8.469	8.637
4340	0.031	9.906	10.176	8.520	8.728
4365	-0.059	9.758	10.008	8.338	8.538
4380	-0.129	9.753	10.010	8.335	8.561
4400	-0.199	9.731	9.996	8.394	8.537
4560	-0.145	9.692	9.963	8.290	8.503
4760	-0.113	9.620	9.890	8.227	8.447
4800	-0.100	9.608	9.874	8.207	8.450
4820	-0.041	9.624	9.872	8.216	8.448
4860	0.124	9.730	9.981	8.301	8.573
4900	-0.015	9.587	9.856	8.188	8.445
4920	-0.072	9.585	9.852	8.186	8.435
4960	-0.079	9.567	9.818	8.166	8.395
5000	-0.070	9.556	9.804	8.154	8.387
5120	-0.045	9.526	9.775	8.116	8.367
5240	-0.023	9.497	9.751	8.080	8.347
5400	-0.003	9.453	9.712	8.033	8.309
5560	0.028	9.427	9.682	8.004	8.288
5760	0.070	9.397	9.653	7.971	8.260
6020	0.131	9.373	9.630	7.943	8.237
6420	0.194	9.325	9.553	7.893	8.205
6460	0.204	9.321	9.580	7.890	8.203
6500	0.220	9.330	9.590	7.894	8.218
6540	0.367	9.371	9.613	7.913	8.233
6560	0.423	9.450	9.681	7.992	8.351
6580	0.419	9.369	9.622	7.932	8.235
6620	0.245	9.330	9.593	7.893	8.224
6660	0.233	9.305	9.570	7.874	8.197
6700	0.239	9.299	9.564	7.869	8.191
6740	0.242	9.294	9.559	7.866	8.188
6780	0.250	9.290	9.555	7.865	8.178
7100	0.310	9.270	9.539	7.849	8.170
7460	0.371	9.255	9.524	7.829	8.164
7780	0.425	9.254	9.515	7.819	8.166
8100	0.463	9.233	9.496	7.793	8.145
8380	0.517	9.226	9.489	7.791	8.143
8780	0.461	9.226	9.489	7.787	8.147
9300	0.495	9.226	9.489	7.783	8.150
9700	0.515	9.225	9.488	7.782	8.153
9940	0.634	9.307	9.570	7.861	8.239
10260	0.609	9.238	9.501	7.791	8.176
10820	0.695	9.250	9.513	7.805	8.195
11140	0.736	9.246	9.509	7.796	8.196
12000	0.860	9.272	9.534	7.809	8.227

TABLE 7. Synthetic magnitudes of the four OG F subdwarfs in the  $AB_{95}$  scheme.

	$u'$	$g'$	$r'$	$i'$	$z'$
BD+17°4708	10.56	9.64	9.35	9.25	9.23
BD+26°2606	10.78	9.89	9.61	9.52	9.50
HD19445	9.08	8.23	7.92	7.82	7.79
HD84937	9.32	8.46	8.23	8.16	8.16

The synthesized broadband SDSS magnitudes of the four subdwarfs are presented in Table 7. A least-squares fit into these values with instrumental magnitudes obtained with the SDSS Monitor Telescope system will define the zero point of the SDSS photometric system.

#### 4. STELLAR COLORS AND TRANSFORMATION TO THE JOHNSON–MORGAN SYSTEM

##### 4.1 Stellar Colors in the SDSS Photometric System

We have calculated expected stellar colors on the SDSS system using the spectrophotometric atlas of Gunn & Stryker (1983). Figure 4 shows the loci of  $u' - g'$  vs  $g' - r'$  colors and  $r' - i'$  vs  $g' - r'$  colors for main sequence stars.

Using this atlas we have studied the effect of the previously discussed filter red leaks. Figure 5 shows the effects of red leaks for the  $u'$  filter. For stars with  $g' - r' \leq +1.4$  the leakage (mostly from wavelengths longer than 10 000 Å) is smaller than 0.02 mag; a larger effect for red stars is due to their very weak  $uv$  flux; on the other hand, errors of 0.02 mag in  $u'$  correspond to trivial temperature or metallicity changes for these stars and demanding high accuracy in this band for very red stars does not make much physical sense. Effects of (infrared) leaks are negligible for the  $g'$ ,  $r'$ , and  $i'$  filters for all ordinary stars.

##### 4.2 Transformations to the Johnson–Morgan–Cousins System

H85 has given, for the first time, the continuous SED of  $\alpha$  Lyr. Although there are small discrepancies between H85 and the Castelli & Kurucz SED, we have attempted to calculate the broadband magnitude of  $\alpha$  Lyr using its continuous SED. The agreement for the  $B$  magnitude between the observed and synthetic values (Table 5) [ $\langle \Delta B \rangle_{\text{synthetic-observed}} = 0.030 \pm 0.007$ ] has also encouraged us to make this attempt. In Table 8 we present  $AB_{95}$  magnitudes of  $\alpha$  Lyr for  $u'$  to  $z'$  colors and for the standard Johnson–Morgan–Cousins (1978) colors in the  $AB_{95}$  scheme. The zero points conventionally adopted for  $\alpha$  Lyr are also given. We note that  $V=0.03$ ,  $U-B=-0.01$ , (Johnson & Morgan 1953),  $V-R_c=0$  and  $R_c-I_c=+0.006$  (Taylor 1986). The difference between the two magnitudes is taken to be the offset between  $AB_{95}$  and the conventional magnitude system in which the average A0 V colors are set equal to zero. In this calculation we adopt the response function  $U_3$  given by Buser (1978),  $Bp(=B_2)$  and  $V$  given by AS69, and  $R_c$  and  $I_c$  given by Bessell (1990).

We have also calculated approximate color transformation equations from the Johnson–Morgan–Cousins system to the SDSS system using synthetic magnitudes from the spectro-

The resulting calibration incorporating this zero-point shift is presented in Table 6, together with that for  $\alpha$  Lyr. Values obtained by linear interpolation are listed when data are not available at the specified wavelength. We designate this the  $AB_{95}$  calibration. The difference between  $AB_{95}$  and  $AB_{79}$  is given in Figs. 3(b) and 3(c) for BD+17°4708 and BD+26°2606. The systematic offset discussed above gives a dominant contribution to the difference.

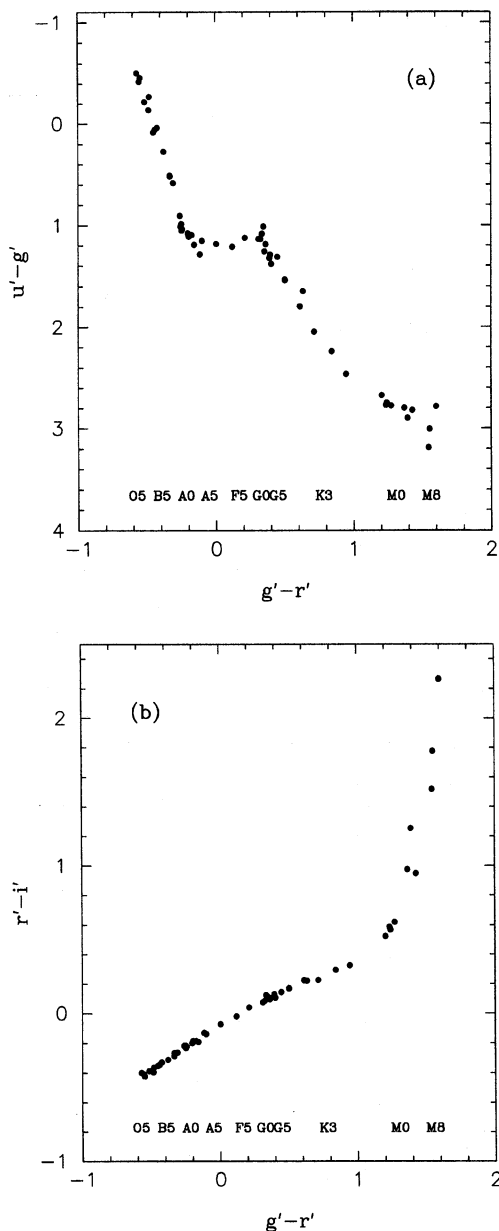


FIG. 4. Colors of main sequence stars in the SDSS photometric system. (a)  $u' - g'$  vs  $g' - r'$  colors, (b)  $r' - i'$  vs  $g' - r'$  colors. Colors are calculated synthetically using the spectrophotometric atlas of Gunn & Stryker.

photometric atlases of Gunn & Stryker (1983) and of Oke (1990). Figure 6 shows color-color plots for the standard versus SDSS colors. We find

$$\begin{aligned}
 g' &= V + 0.56(B - V) - 0.12, \\
 r' &= V - 0.49(B - V) + 0.11, \\
 r' &= V - 0.84(V - R_c) + 0.13, \\
 u' - g' &= 1.38(U - B) + 1.14, \\
 g' - r' &= 1.05(B - V) - 0.23,
 \end{aligned}
 \tag{23}$$

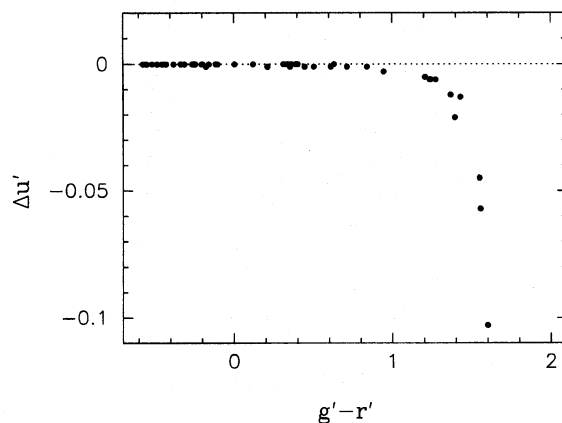


FIG. 5. Effect of filter red leaks for the  $u'$  filter for main sequence stars given in the Gunn-Stryker spectrophotometric atlas.

$$\begin{aligned}
 r' - i' &= 0.98(R_c - I_c) - 0.23 \quad (R_c - I_c < +1.15) \\
 &= 1.40(R_c - I_c) - 0.72 \quad (R_c - I_c \geq +1.15), \\
 r' - z' &= 1.59(R_c - I_c) - 0.40 \quad (R_c - I_c < +1.65) \\
 &= 2.64(R_c - I_c) - 2.16 \quad (R_c - I_c \geq +1.65),
 \end{aligned}$$

which are valid for stars with  $B - V \leq +1.5$ . We applied these relations to the  $UBVR_c I_c$  photometry data (Turnshek *et al.* 1989) for 4 OG subdwarfs and 23 dwarfs given in Oke (1990), and compared the transformed  $u' g' r' i'$  magnitudes with those directly obtained from the synthetic magnitude calculations using the spectrophotometry of Oke (1990). The differences are again reasonably small:  $\Delta_{\text{syn-transformed}} g' = 0.03 \pm 0.03$ ,  $\Delta_{\text{syn-transformed}} (u' - g') = 0.02 \pm 0.05$ ,  $\Delta_{\text{syn-transformed}} (g' - r') = 0.03 \pm 0.04$ ,  $\Delta_{\text{syn-transformed}} (r' - i') = 0.03 \pm 0.02$  (excluding LT9491 for which the two magnitudes are discrepant by more than 1 mag; one of the catalogs is obviously in error).

## 5. IMPLEMENTATION OF THE SDSS SYSTEM

The photometric system is defined by the camera at the SDSS Monitor Telescope, which consists of a single thinned UV-antireflection coated, back-illuminated  $2048 \times 2048$  CCD and the five filters discussed in this paper. The telescope is a conventional two-mirror Ritchey-Chrétien Cassegrainian with a corrector whose transmission has negligible effect on the color system. The survey camera installed on the 2.5 m telescope consists of 30  $2048 \times 2048$  CCDs, mosaicked on the focal plane. Among 30 detectors, 6 are UV-antireflection-coated thinned devices (for  $u'$ ), 18 are normal antireflection-coated thinned devices (for  $g'$ ,  $r'$ , and  $i'$ ), and remaining 6 for the  $z'$  band are conventional thick, front-illuminated

TABLE 8. Magnitudes of  $\alpha$  Lyr in the  $AB_{95}$  and the conventional schemes.

	$u'$	$g'$	$r'$	$i'$	$z'$	$U$	$B$	$V$	$R_c$	$I_c$
$AB_{95}$	0.981	-0.093	0.166	0.397	0.572	0.719	-0.120	0.019	0.212	0.453
conv.						0.02	0.03	0.03	0.03	0.024

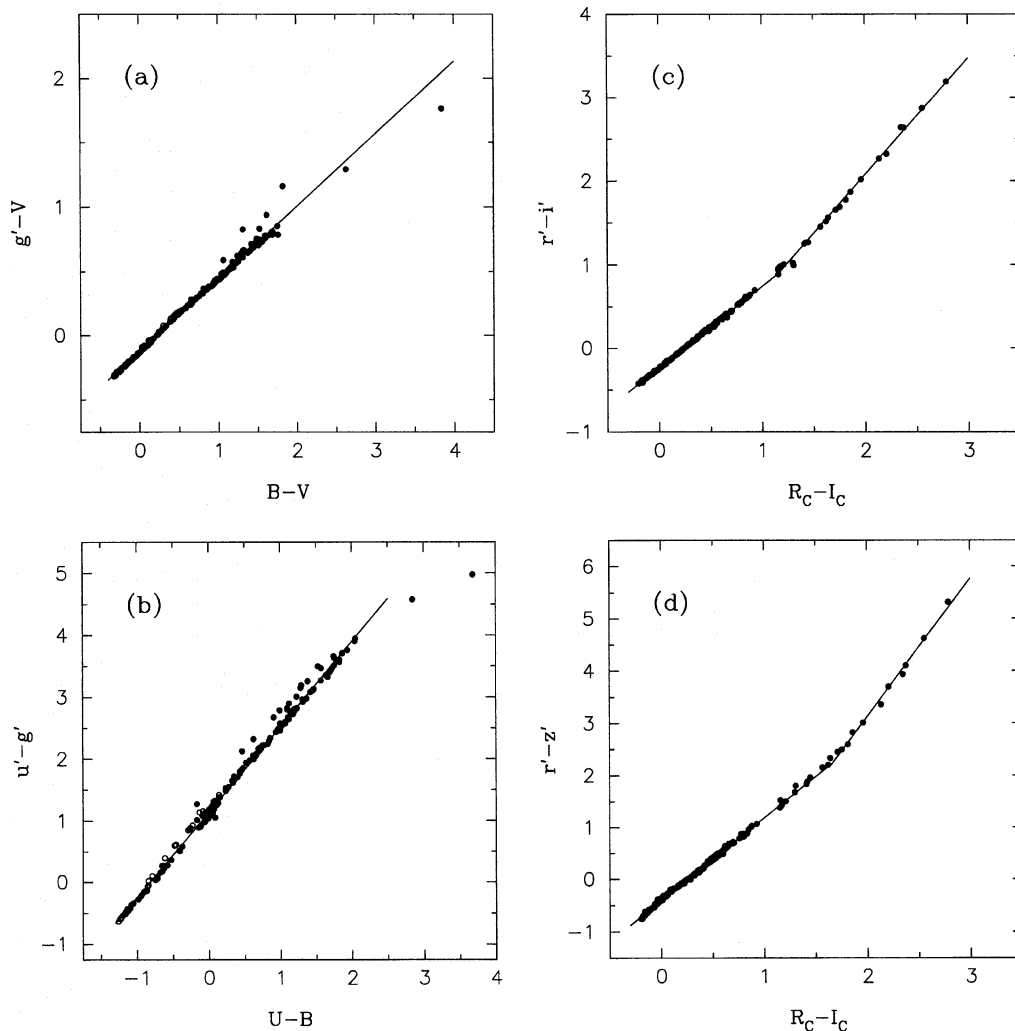


FIG. 6. Stellar colors in the SDSS system vs the standard Johnson-Morgan-Cousins system. (a)  $B-V$  vs  $g'-V$ , (b)  $U-B$  vs  $u'-g'$ , (c)  $R_c-I_c$  vs  $r'-i'$ , and (d)  $R_c-I_c$  vs  $r'-z'$ . The atlases of Gunn & Stryker (1983) (solid circles) and Oke (1990) (open circles) are used. The clearly defined second sequence in (b) consists of late M stars which have similar ultraviolet colors to late K and early M stars but very different detailed spectra.

devices. The color response of the survey camera therefore differs slightly from that of the Monitor Telescope, most significantly in the  $g'$  band, where the response shapes are noticeably different (see Fig. 7). We also find that the quantum efficiencies of the state-of-the-art thinned devices vary somewhat from CCD to CCD. In order to correct the offset of the instrumental magnitudes obtained with the 30 CCDs relative to that defined with the Monitor Telescope system, we will introduce 30 color-color relations that will be established through the observation of standard stars and applied to the magnitudes to be published in the SDSS catalogs. Figure 7 shows typical response functions for the survey camera, compared with those of the Monitor Telescope (Fig. 2). The color offset between the two systems amounts to as much as  $\pm 0.02$  mag if it is not corrected with color-color relations. After correction accuracies of 0.005 mag should be attainable except for very red M stars for which no broadband

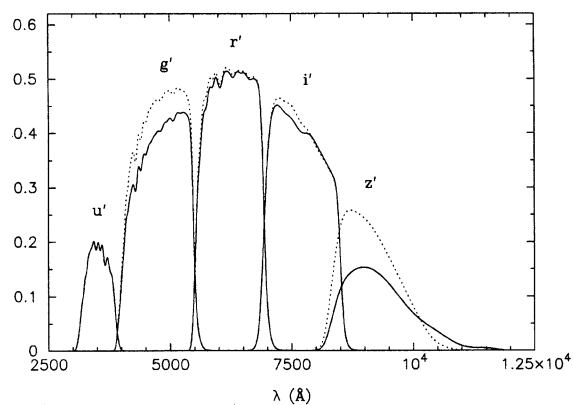


FIG. 7. Response function of the SDSS survey camera (solid curves), as compared with that of the Monitor Telescope (dashed curves), which defines the SDSS photometric system. The two curves are nominally identical for the  $u'$  band.



color relations work well because of the complexity of their spectra.

Finally, we remark that the magnitudes we use in this project (primed magnitudes) directly represent  $AB$  values if one calculates the effective frequency of the bands via the relation  $\delta\lambda_{\text{eff}} = \lambda_{\text{eff}} \sigma^2 \delta n$  as discussed below Eq. (5).

This work was done as a part of the Sloan Digital Sky Survey Project. We would like to pay tribute to Bev Oke for his three decades of effort in developing the  $AB$  spectrophotometric system: this fundamental program provided much of

the foundation for the work presented in this paper. We also thank Don York for his encouragement for this work and Bev Oke for a number of valuable suggestions improving the manuscript. This work was partially supported by Grant-in-Aid of the Ministry of Education of Japan (05101002) and by a Grant NSF No. AST91-00121 (JEG). J.E.G. also thanks Japan Society for Promotion of Science for support. M.F. wishes to acknowledge support from the Fuji Xerox Corporation.

#### REFERENCES

- Azusienis, A., & Straizys, V. 1969, *AZ*, 13, 316 (AS69)  
 Bessell, M. S. 1990, *PASP*, 102, 1181  
 Buser, R. 1978, *A&A*, 62, 411  
 Castelli, F., & Kurucz, R. L. 1994, *A&A*, 281, 817  
 Cousins, A. W. J. 1978, *MNASSA*, 37, 8  
 Gunn, J. E., & Stryker, L. L. 1983, *ApJS*, 52, 121  
 Hass, G. 1965, in *Applied Optics and Optical Engineering*, Vol. III, edited by R. Kingslake (Academic, New York), pp. 309–330  
 Hayes, D. S. 1985, *Calibration of Fundamental Stellar Quantities*, in *IAU Symposium No. 111, Stellar Quantities*, edited by D. S. Hayes *et al.* (Reidel, Dordrecht), p. 225 (H85)  
 Hayes, D. S., & Latham, D. W. 1975, *ApJ*, 197, 593  
 Johnson, H. L., & Morgan, W. W. 1953, *ApJ*, 117, 313  
 Magrath, B. 1994, *CFHT Information Bull.* 30, 15  
 Mermilliod, J.-C. 1991, *Photoelectric Photometry Catalogue of Homogeneous Measurements in the UBV System* (NASA Goddard Space Flight Center)  
 Oke, J. B. 1990, *AJ*, 99, 1621  
 Oke, J. B., & Gunn, J. E. 1983, *ApJ*, 266, 713 (OG)  
 Oke, J. B., & Schild, R. E. 1970, *ApJ*, 161, 1015  
 Schneider, D. P., Gunn, J. E., & Hoessel, J. G. 1983, *ApJ*, 264, 337  
 Shiles, E., Sasaki, T., & Smith, D. 1980, *Phys. Rev. B* 22, 1612  
 Taylor, R. J. 1986, *ApJS*, 60, 577  
 Thuan, T. X., & Gunn, J. E. 1976, *PASP*, 88, 543  
 Turnshek, D. E., *et al.* 1989, *Standard Astronomical Sources for HST: 2—Optical Calibration Targets* (STScI)  
 Wade, R. A., Hoessel, J. G., Elias, J. H., & Huchra, J. P. 1979, *PASP*, 91, 35